

Characterizing high and low accretion states in VY Scl CVs using ZTF and *TESS* data

C. Duffy¹,^{1,2,3}★ Kinwah Wu¹,⁴ G. Ramsay¹,² Matt A. Wood⁵ Paul A. Mason^{6,7} Pasi Hakala⁸ and D. Steeghs¹

¹Department of Physics, Lancaster University, Lancaster LA1 4YB, UK

²Armagh Observatory and Planetarium, College Hill, Armagh BT61 9DB, Northern Ireland, UK

³Department of Physics, University of Warwick, Gibbet Hill Road, Coventry CV4 7AL, UK

⁴Mullard Space Science Laboratory, University College London, Holmbury St. Mary, Surrey RH5 6NT, UK

⁵Department of Physics & Astronomy, Texas A&M University, Commerce, TX 75429-3011, USA

⁶Department of Science, New Mexico State University, MSC 3DA, Las Cruces, NM 88003, USA

⁷Picture Rocks Observatory, 1025 S. Solano Dr Suite D., Las Cruces, NM 88001, USA

⁸Finnish Centre for Astronomy with ESO (FINCA), Quantum, University of Turku, Vesilinnantie 5 FI-20014, Finland

Accepted 2024 October 24. Received 2024 October 18; in original form 2024 July 5

ABSTRACT

VY Scl binaries are a sub-class of cataclysmic variable (CV) which show extended low states, but do not show outbursts which are seen in other classes of CV. To better determine how often these systems spend in low states and to resolve the state transitions we have analysed Zwicky Transient Facility (ZTF) data on eight systems and Transiting Exoplanet Survey Satellite (*TESS*) data on six systems. Half of the sample spent most of the time in a high state; three show a broad range and one spends roughly half the time transitioning between high and low states. Using the ZTF data, we explore the colour variation as a function of brightness. In KR Aur, we identify a series of repeating outburst events whose brightness appears to increase over time. Using *TESS* data, we searched for periods other than the orbital. In LN UMa, we find evidence for a peak whose period varies between 3 and 6 d. We outline the current models which aim to explain the observed properties of VY Scl systems which includes disc irradiation and a white dwarf having a significant magnetic field.

Key words: accretion, accretion discs – binaries: general – stars: magnetic field – novae, cataclysmic variables – stars: variables: general.

1 INTRODUCTION

Cataclysmic variables (CVs) are interacting binaries with a white dwarf (WD) accreting material from, usually, a late type (donor) star (see Warner 2003, for a review). Mass transfer in CVs occurs via Roche lobe overflow from the donor star through the inner Lagrangian (L1) point of the binary. If the WD is modestly magnetized ($B \lesssim 0.1$ MG), an accretion disc can be formed, mediating material inflow on to the WD via a boundary layer. CVs often show high- and low-optical states. Except for Polars, which are discless CVs containing a highly magnetic WD, the two states correspond respectively to a hot, bright disc with high viscosity and a cool, faint disc with a low viscosity (see Cannizzo 1993). According to the Disc Instability Model (DIM; for a review see Hameury 2020), the existence of state bimodality and state transitions are associated with CV outbursts, where one or more physical parameters of the accretion disc changes in such a manner as to make the disc unstable, which results in an abrupt increase in the mass accretion on to the WD. The long-term behaviour of mass transfer in CVs and the (in)stability

of their accretion discs provides insight into the accretion and mass transfer processes in general and the nature of viscosity that drives the accretion flow (Warner 2003).

VY Scl binaries, also known as ‘anti-dwarf novae’, are a subclass of the non-magnetic CVs. They are distinguished from nova-like systems, which have a high mass transfer rate, as their optical brightness can decrease by several magnitudes for up to several 100 d at a time (Warner 2003). The drop in the brightness reflects the decrease in the accretion flow on to the WD, which is attributed to the decrease in the mass-transfer rate, with possibly even a temporary cessation of mass transfer from the secondary star in some systems. Noticeably, VY Scl binaries have not been observed in outburst, despite the DIM predicting that outbursts should occur in their low state (Leach et al. 1999). However, lower amplitude ‘stunted’ outbursts have been observed in some VY Scl binaries during their high states (e.g. Honeycutt, Kafka & Robertson 2014).

Various models have been proposed to explain the occurrence of low states in CVs, with star-spot models amongst them. In semidetached binaries such as CVs, where the rate of mass transfer is determined by the physical condition of the low-mass donor star at the L1 point, the gas temperature and the atmospheric pressure scale heights are two core parameters (Lubow & Shu 1975). Low-mass

* E-mail: c.j.duffy@lancaster.ac.uk

stars are often magnetically active, with some showing coronal flares and also migrating star-spots. The passing of star-spots to regions close to the L1 point would lead to a reduction in gas temperatures and atmospheric pressure scale height, which in turn modifies the mass transfer rate (see Livio & Pringle 1994).

The star-spot models highlight the importance of stellar magnetism in regulating the mass transfer in low-mass semidetached binaries, and it is a starting point for building more holistic models, such as those invoking a magnetic valve mechanism (e.g. Wu & Kiss 2008; Duffy et al. 2022; Mason et al. 2024), where the magnetic interactions between the WD and the companion star control mass transfer in the binary. This provides a unified description for high and low states, the state transition and the duty cycles in some CV sub-classes, in particular the Polars, covering both systems with low and high WD magnetic fields ($B \sim 10\text{--}200$ MG; Mason et al. 2024).

While there is evidence that the magnetic valve mechanism can explain high/low states in Polars (Mason et al. 2022), in the same form it is clearly inapplicable to the non-magnetic VY Scl binaries. However, such a scenario in VY Scl binaries would rely solely on the atmospheric magnetic activity of the low-mass companion star. We note that what drives the state transition, sustains the mass transfer during the high state and halts the mass transfer during the low state would also depend additionally on the mechanical and thermal conditions of the low-mass donor star, as well as the orbital dynamics of the binary.

With the exception of Polars, CVs possess an accretion disc. During the low state the accretion disc is expected to be cool. It may evolve in such a way that a disc instability develops, triggering outbursts (see e.g. Cannizzo 1993). The lack of outbursts observed in VY Scl binaries suggests that some mechanism(s) are present which inhibit disc instability. Leach et al. (1999) proposed that the anticipated outbursts are suppressed by a high WD atmospheric temperature ($\sim 40\,000$ K), which heats the inner disc and thus prevents the development of the instability needed for outburst. This proposition is consistent with observations of the WDs in some VY Scl binaries which are found to be relatively hot (see e.g. Mizusawa et al. 2010). Whilst it has explained the absence of outbursts in the low state, it is yet to account for the lack of outbursts in the transition between the low and high states, known as the intermediate state, (see e.g. Leach et al. 1999; Zemko et al. 2014), which is observed in some systems. The durations of these intermediate states are longer than the viscous time-scale, and as the accretion disc is in an unstable configuration, the DIM would predict outbursts to occur.

In order to explain the general absence of outbursts, Hameury & Lasota (2002, 2005) proposed that the magnetic field of the WDs in VY Scl binaries are strong enough to affect the accretion flow. They showed that a relatively weak magnetic field ($B \sim 40$ kG) is sufficient to prohibit the formation of a low-state accretion disc around a WD of $\sim 0.7 M_{\odot}$. For a similar system, a WD magnetic field $B \gtrsim 6$ MG would be sufficient to disrupt the disc during the majority of the intermediate state so that outbursts would not be possible. Such a WD magnetic field strength would place the binaries into the CV sub-class Intermediate Polars, whose WDs generally have a magnetic field of $10\text{ MG} \gtrsim B \gtrsim 0.1\text{ MG}$.

The absence of a full-scale accretion disc, proposed by Hameury & Lasota (2002, 2005), was used to explain the absence of outbursts in the low state of VY Scl binaries. A more extreme proposal is that the accretion disc is entirely absent in the low state due to a complete cessation of mass transfer. Whilst the enhanced magnetic fields associated with star-spots migrating to the L1 region can temporarily halt the mass outflow from the donor star, it is hard to sustain for a prolonged time unless an external force e.g. the WD magnetic field in the magnetic valve scenario for Polars described in Duffy

et al. (2022) and Mason et al. (2024) is present to prevent the star-spots migrating out of the L1 region. However, if the mass transfer process is intrinsically unstable, the binary can enter a prolonged low state where mass transfer ceases and a full-scale accretion disc is naturally absent. The study of Wu, Wickramasinghe & Warner (1995) has shown that irradiative heating feedback can trigger such mass transfer instabilities.

Attempts have been made to verify the star-spot and the magnetic disc disruption scenarios, but the situation is complicated by the fact that whilst some observations support one or other of the scenarios, other observations disprove them. The study of MV Lyr by Linnell et al. (2005), for example suggests that neither the star-spot nor the disc-disruption scenario is applicable with the WD and/or the inner disc being too cool and also showing no evidence of a WD magnetic field of sufficient strength. On the other hand, the absence of the accretion disc in TT Ari (Gänsicke et al. 1999) would favour the magnetic disc-disruption scenario. Similarly, Medina Rodriguez et al. (2023) found that during low states SDSS J154453.60+255348.8 did not show evidence for an accretion disc, which supports the predictions of Hameury & Lasota. However, when looking at VY Scl, the sub-class archetype, Schmidtobreick et al. (2018) found evidence of an accretion disc during the low state, and they also used this to rule out the disc-disruption scenario.

Despite VY Scl binaries generally not outbursting during their low states, ‘stunted’ outbursts were identified by Honeycutt & Kafka (2004) in FY Per and V794 Aql during their low states. These stunted outbursts have greatly reduced amplitude compared with those which would be expected from an outburst in similar non-VY Scl systems. Schmidtobreick et al. (2018) also found aperiodic variations in the brightness of VY Scl itself, and suggested that they are a similar phenomenon. The nature of stunted outbursts is unclear: they could be associated with certain disc instabilities, or alternatively fluctuations in mass transfer rates, or a combination of both (Honeycutt, Robertson & Turner 1998; Honeycutt 2001). These outbursts require the accretion disc to act as an agent, and thus they would exclude the possibility of a strongly magnetized WD. Magnetically gated outbursts have also been observed in MV Lyr (Scaringi et al. 2017) from which they inferred a WD magnetic field of similar magnetic to those proposed by Hameury & Lasota (2002, 2005).

In this paper, we investigate the long-term behaviour of eight VY Scl binaries using the multicolour photometric data from the Zwicky Transient Facility (ZTF; Bellm et al. 2019) in order to better understand the long term behaviour of eight VY Scl binaries and therefore the underlying processes that give rise to the observed high and low accretion states, and their duty cycles. We use also extended optical photometric data from the Transiting Exoplanet Survey Satellite (*TESS*; Ricker et al. 2015) to search for periods longer than the orbital period and resolve transitions between high and low states.

2 PHOTOMETRIC DATA

We searched the ZTF and *TESS*¹ light curves of all known VY Scl systems and found 10 systems which showed features such as transitions or short duration brightenings, as detailed in Table 1.²

¹The sources in this paper were included on the 20 s or 2 min cadence list thanks to their inclusion on the following Guest Investigator programmes: G022071/PI Scaringi; G022208/PI Zakamska; G022116/PI Schlegel; G022141/PI Barlow; G022254/PI Sion; G03071/PI Scaringi; G03044/PI Scaringi; G04208/PI Littlefield; and G04046/PI Scaringi.

Table 1. List of sources analysed in this work, detailing the feature of interest to this work and the origin(s) of the data considered for the analysis. Features; transitions, ‘outburst’, and superorbital periods are denoted by T, O, and S, respectively.

Source	Orbital period (min)	Feature(s)	High state (per cent)	Mean low state depth (mag)	ZTF	TESS
RX J2338+431	187.7 ^a	T	93.5	3.1	✓	✓
MV Lyr	191.4 ^b	T	81.0*	5.0	✓	✓
TT Ari	198.1 ^c	S	N/A	N/A	×	✓
LN UMa	207.9 ^d	O, P	N/A	N/A	✓	✓
V794 Aql	220.8 ^e	T, O	83.1**	2.8	✓	×
BZ Cam	221.3 ^f	T, O	90.2	0.7	✓	✓
ES Dra	225.6 ^g	T, O	90.0	1.4	✓	×
KR Aur	234.4 ^h	T, O	35.4	4.6	✓	×
V504 Cen	252.8 ⁱ	S	N/A	N/A	×	✓
MP Gem	Unknown	T	74.4*	4.0	✓	×

Notes. Citations:^a Weil, Thorstensen & Haberl (2018), ^bSkillman, Patterson & Thorstensen (1995), ^cWu et al. (2002), ^dHillwig, Robertson & Honeycutt (1998), ^eHoneycutt et al. (1998), ^fPatterson et al. (1996), ^gRingwald & Velasco (2012), ^hShafter (1983), ⁱBruch (2022).

* These systems have visibility gaps during the majority of the suspected low state times, leading to artificially inflating the per cent high state. Estimated points filling in the established low state at the same cadence as the observations were inserted for these systems in order to calculate these values, without these estimated points the values are MP Gem: 91.3 per cent and MV Lyr: 88.7 per cent.

** The high state in V794 Aql was defined as those points brighter 1 mag below the mean high state brightness, in order to account for the high brightness variability seen in the high state of this system. Using the definition applied to other systems yields a value of 49.3 per cent.

N/A denotes systems where no low states are seen in the data considered, however, as known VY Scl systems it would be incorrect to record a 100 per cent high state.

The ZTF data on these systems, shown in Fig. 1, was collected to allow us to probe the longer term behaviour seen in these systems, quantifying the occurrence and duration of the features of interest. The TESS photometry of these systems allows us to probe their short term behaviour, which gives us a more precise understanding of the processes at work in these features.

ZTF is a time domain survey programme using the Palomar 1.2 m telescope, which is capable of covering $47^{\circ}2$ per exposure. As such ZTF is capable of surveying the entire sky rapidly, providing photometry on a diverse number of sources with a limiting brightness of mag ~ 20 . ZTF operates a number of different survey programmes including the public survey which accounts for 50 per cent of the observation time. The public survey makes observations in two filters ZTF-*g* and ZTF-*r*, $\sim 4087\text{--}5522$ and $\sim 5600\text{--}7316$ Å, respectively (see Bellm et al. 2019, for a full description of ZTF operations). We downloaded ZTF photometry from the NASA/IPAC archive.³ The data used has been processed through the standard ZTF pipeline, where each photometric point is assigned a quality flag, `catflags`. Only data with `catflags` = 0 were included in analysis.

TESS is a space observatory launched in 2018. It makes observations of pre-defined sectors using four wide field telescopes, each with a $24^{\circ} \times 24^{\circ}$ field of view. Each sector lasts for 27 d and is near continuous, with a short mid-point break for data transmission and momentum unloading, and generates 20 s (from the first extended mission onwards) and 120 s cadence photometry on a list of pre-defined targets (see Ricker et al. 2015, for full details of the TESS mission). We downloaded the calibrated light curves of all sources from the MAST data archive.⁴ We used the data values for `PDCSAP_FLUX`, which are the simple aperture photometry values, `SAP_FLUX`, after the removal of systematic trends common to all stars in that chip. Each photometric point is assigned a `QUALITY`

flag which indicates if the data has been compromised to some degree by instrumental effects. We removed those points which did not have `QUALITY` = 0 and normalised each light curve by dividing the flux of each point by the mean flux of the star.

2.1 Analysis

To investigate the variation in state behaviour and transitions over the duration of observations, we quantified the distribution of the brightness states in the systems where we saw both high and low states. Histograms showing the number of days a given brightness bin occurs in the ZTF *g*-band light curves are shown as part of Fig. 2. Although this allows for a good visual interpretation of the distribution of brightness states it does have limitations. It is heavily dependent on the sampling of the different states, e.g. for MV Lyr, although the light curve indicates the presence of a ~ 200 d low state as this occurs during a visibility gap it is underrepresented by the histogram. Despite this, we used these to quantify the fraction of time that a system occupies a high state as shown in Table 1. This was completed by visually identifying a section of a system’s light curve which corresponded the high state and using this section to determine a mean high state brightness. The high state was then defined to be when the light curve was no fainter than 0.5 mag below the mean high state brightness. Using 1D histograms (although with 100 bins instead of 10 bins as shown in Fig. 2), we were subsequently able to determine the distribution of brightness within the light curve and thus the fraction of time each binary spent in a high state. This shows that for most cases in which we see a transition it spends ~ 90 per cent of the time in a high state, except KR Aur where the duty cycle is only ~ 35 per cent.

We have quantified the behaviour of the transitions seen in each of the ZTF data sets by calculating the *e*-folding time value,⁵ τ , for each, which gives us a metric with which to describe the rate of change of brightness (or ‘speed’) of the transition. We have tabulated the

²We initially accessed photometry on 23 known or suspected VY Scl systems, those which did not show events of interest pertinent to this work were excluded from further consideration This included BH Lyn and LX Ser in which eclipses were visible in the TESS data.

³<https://irsa.ipac.caltech.edu/Missions/ztf.html>

⁴<https://archive.stsci.edu/teess/>

⁵ τ is the value describing time required for the brightness to change by a factor of *e* and is given by the expression $(\log_{10} e/0.4)/(\Delta m/\Delta t) = 1.086/(\Delta m/\Delta t)$ (Honeycutt & Kafka 2004).

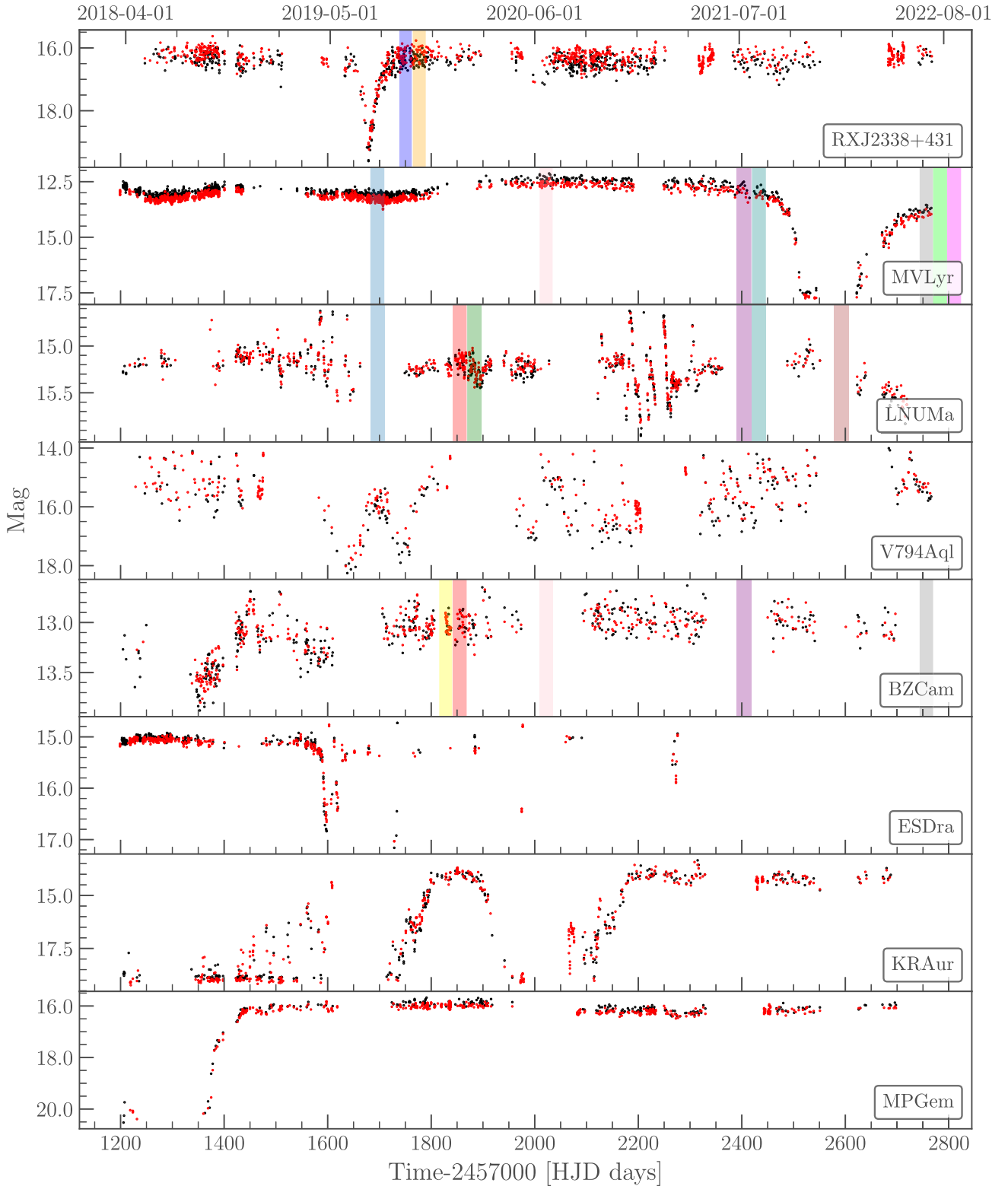


Figure 1. The ZTF light curves of the eight sources which were found to show features of interest. Black and red data points denote ZTF-*g* and ZTF-*r* data, respectively. The windows denote the times of *TESS* observations with colours indicating the sector; blue – s14, dark blue – s16, orange – s17, yellow – s19, red – s20, green – s21, pink – s26, purple – s40, teal – s41, brown – s47, grey – s53, lime – s54, fuchsia – s55. Group A systems: RX J2338+432, MV Lyr, ES Dra, KR Aur, and MP Gem. Group B systems: LN UMa, V794 Aqr, and BZ Cam. (see Section 4.1).

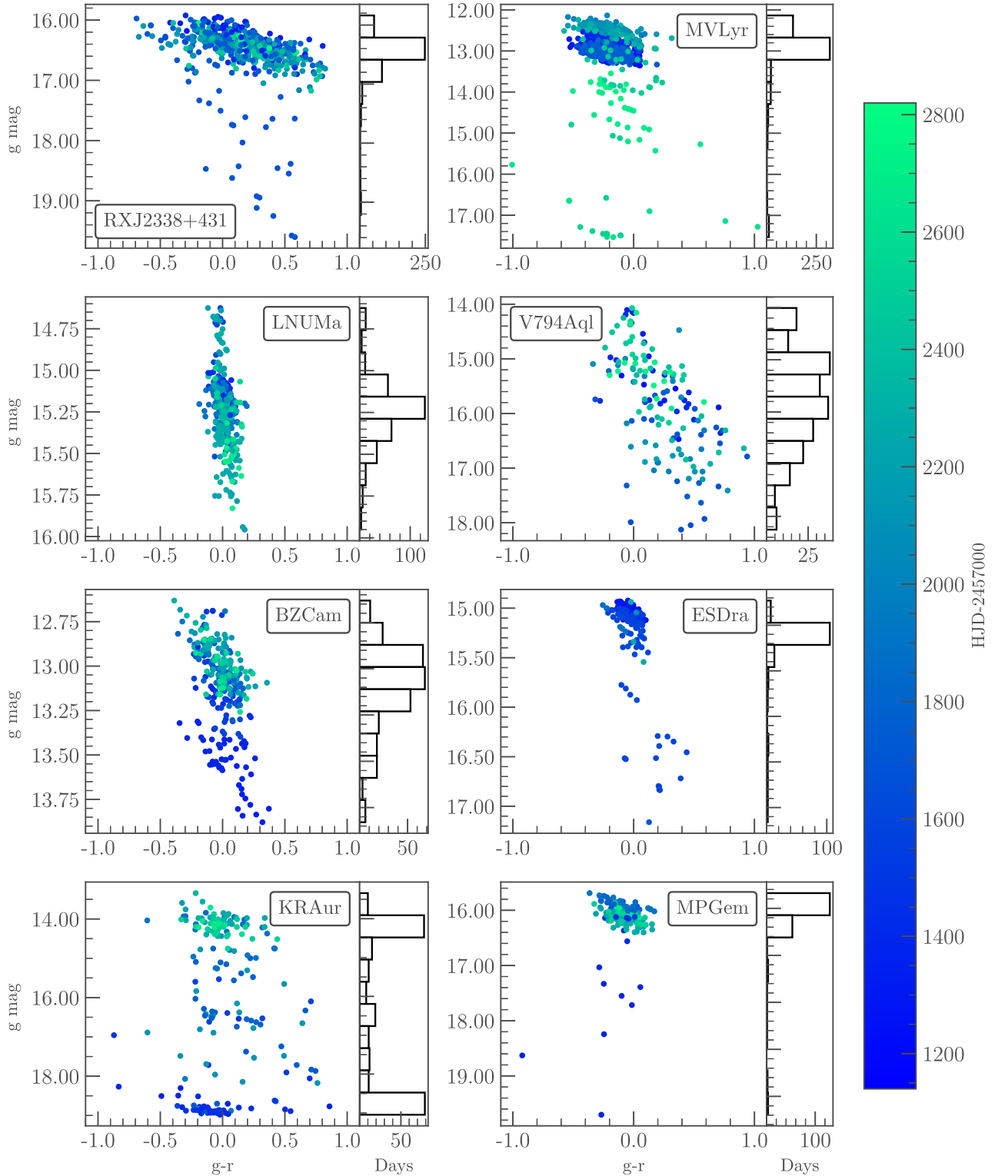


Figure 2. The ZTF colour-magnitude diagrams of each of the ZTF sources. Each datum has been coloured according to the associated g -band observation time using the same time range as seen in Fig. 1. Attached to each colour magnitude is a histogram showing the number of days in which observations in a given g -band brightness bin were made. Errors on the magnitude and colour index were calculated, though in almost every case were contained entirely within the size of the marker.

results of this calculation in Table 2. Together with quantifying the duty cycle discussed above these metrics allow us to quantitatively discuss the nature of the different states and transitions seen in the VY Scl binary population.

As ZTF provides colour information from multiband observations, it is possible to use these data in order to probe the colour evolution of these systems during different states or at singular moments in time. We show in Fig. 2 colour-magnitude diagrams for each of the systems

Table 2. The e -folding time of each of the transitions in each of the sources seen to transition in ZTF. Type refers to the direction of transition, with + denoting a transition from low to high state and – denoting a transition from high to low state. Times are given in HJD-2457000.

Source	Start (HJD)	End (HJD)	Type (+ / –)	τ (d)
RX J2338+431	1650	1678	–	12.2
	1679	1720	+	17.0
MV Lyr	2401	2517	–	50.8
	2622	2765	+	46.0
V794 Aql	1582	1637	–	24.9
	1640	1693	+	23.3
	1694	1743	–	32.1
	1747	1792	+	19.3
BZ Cam	1343	1434	+	160.8
ES Dra	1573	1598	–	17.0
KR Aur	1716	1837	+	24.6
	1880	1956	–	16.7
	2112	2204	+	25.0
MP Gem	1125	1222	–	33.5
	1360	1444	+	25.6

Note. The first transition in MP Gem is measured with additional data from AAVSO.

for which we have ZTF data. In each the data have been coloured such that the time of observation can be compared with a source’s parent light curve. This shows that many are well constrained in colour, with both low and high states recording similar colour indices with no apparent preferences to the time of observation. There are, however, some exceptions to this – e.g. V794 Aql shows a trend to increased redness as it becomes fainter.

In order to probe periodic features in both ZTF and *TESS* data, we used Lomb–Scargle periodograms as developed by *Astropy* and implemented in *Lightkurve* (Lomb 1976; Scargle 1982; *Astropy* Collaboration 2013, 2018, 2022; *Lightkurve* Collaboration 2018). Comparing periodograms allowed us to identify a range of periodic features present in both data sets, which gives us insight into the processes taking place. Although much of the *TESS* data reveal periodic behaviour, it is often the known orbital period.

As can be seen in Fig. 1, there is evidence of a number of short duration brightness events taking place across various objects. As we see substantial variation in the manifestation of these events, our approach to studying them must reflect this individuality. Specifically, we consider the duration and recurrence time of these events, their temporal profile, and if possible their the colour index. This allows us to characterise these events and establish the physical processes which underpin them.

2.2 Individual systems

Although our aim is to explore the features of VY Scl systems as a whole, we first discuss briefly the behaviour of individual systems. Here, we focus on those systems observed by ZTF in Fig. 1, as these data illustrate the long term behaviour of the systems to be considered and where appropriate is compared and contrasted with shorter term, higher cadence observations from *TESS*.

2.2.1 RX J2338+431

Initially seen in the previously reported high state (Weil et al. 2018), the ZTF data show a single, short, low state, that does not plateau at a low state brightness, but instead almost immediately begins a transition back to the high state. The system remains at a brightness

minimum for at most 5 d with the entire episode lasting at most 80 d. Although visually appearing similar to other events presented, the transitions in J2338 are some of the fastest we have observed. The high states outwith the episode are unremarkable with only a small (mag ~ 0.5) variation in brightness consistent with a combination of observational effects and orbital variability. J2338 does not show a robust variation in colour behaviour between low and high state – although there is a slight lean towards reddening in the low state, but the short nature of the transitions and low state make it difficult to confirm. Despite this, J2338 shows the greatest variation in colour index of any of the systems which we consider here.

The *TESS* data available for this binary catch only the very end of the transition out of the low state and mostly cover the second high state. As such these are not a particularly useful resource for considering the low state or the transition therein. The coverage from *TESS* indicates that the newly established high state is uneventful.

2.2.2 MV Lyr

In MV Lyr, we observe a single low state at a brightness of mag ~ 17.5 which lasts ~ 200 d: this is consistent with low states previously seen (Scaringi et al. 2017), who also identified magnetically gated outbursts during low states in MV Lyr. The vast majority of the low state occurs during a visibility gap so we are unable to report on its features, including any possible missed outbursts. The transitions which we measure in MV Lyr are at the slower end of the measured distribution, in part this may be associated with the depth of the low state relative to the other system considered here. Outwith the low state we see MV Lyr in a high state where the brightness appears to vary over ~ 400 d between mag ~ 12.5 and 13.5. Despite this, the shorter term variation on the order of a few days is minimal and entirely in line with expectations of a locally stable high state. MV Lyr shows a relatively narrow spread of colour indices which remains mostly consistent between the high and low states, perhaps becoming slightly redder through the low state. We additionally see some outliers as seen in Fig. 2 but we believe that these can be discounted as spurious.

The *TESS* observations of MV Lyr are almost entirely from the high state and provides a steady state light curve. Despite this *TESS* does appear to confirm the long term variability seen by ZTF with successive sectors varying in flux at a pattern that matches the ZTF observations.

2.2.3 TT Ari

TESS 20 s photometry of TT Ari is available in two successive sectors during the high state. In the power spectrum (Fig. 3), we observe the known orbital period variation (0.14 d), and periods of 0.15 and 0.13 d which are the known positive and negative superhumps Bruch (2022). We also see a longer term variation of ~ 0.3 mag in the light curves. This was revealed in our period searching to be a 1.1 d period with a power between 0.5 and 0.75 d^{-1} that of the orbital period. This period was also found by Bruch (2022) who identified it as a beat between the superhump periods which originates from the modulation of the negative superhump on the disc precession period. This precession period does not appear in the power spectra of this system but using equation (1) in Wood, Thomas & Simpson (2009) which relates the precession period to the positive superhump period and the orbital period we find an expected prograde precession period of 1.54 d. Long term study of TT Ari by Bruch (2019)

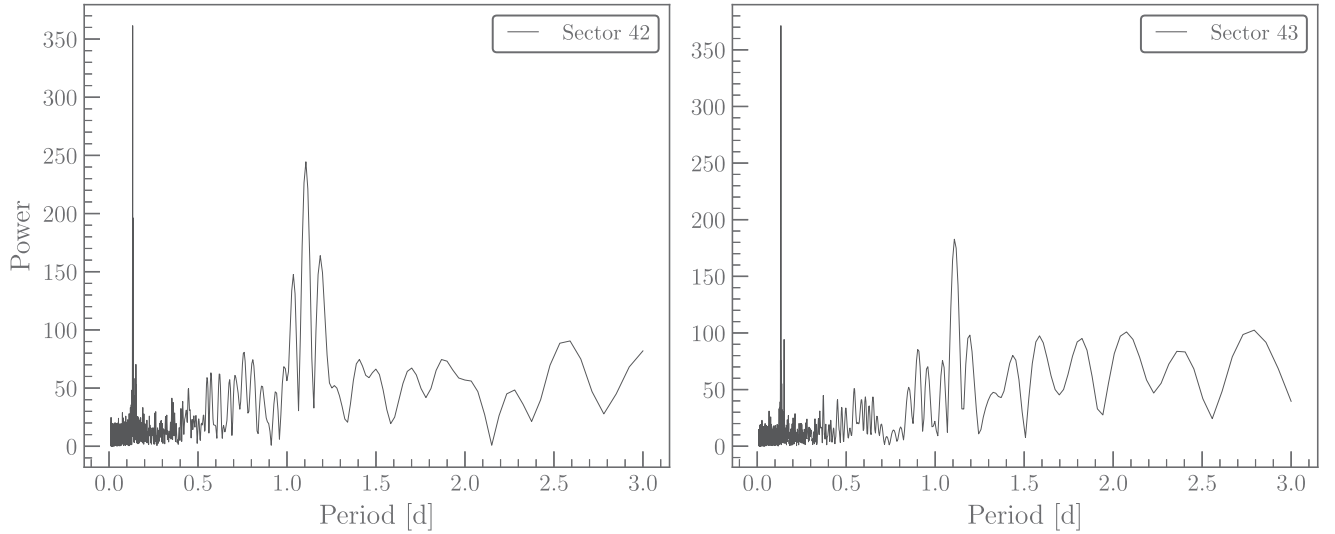


Figure 3. The Lomb–Scargle periodograms of both of the *TESS* sectors of TT Ari observations showing the the beat (disc precession) period at 1.1 d, the strongest peak in both is the orbital period.

identified a number of (quasi) periodic features, including a quasi-periodic oscillation during the high state, between 18 and 25 min; despite this we have been unable to identify a similar feature in the *TESS* data.

2.2.4 LN UMa

Throughout the ZTF observations, LN UMa is found in a high state with the majority of observations taking place at mag ~ 15.25 , which is the known high state brightness (Papadaki et al. 2009). Despite this long running high state, we see a number of short-lived events wherein the brightness abruptly falls by as much as 0.75 mag in fewer than 10 d. It then subsequently rises over ~ 5 d to ~ 0.5 mag brighter than the established high state before dimming over ~ 20 d (see Fig. 1). These events often occur in clusters with 4 or 5 seen in a ~ 150 d time span, and as such one event may flow directly into the next. We believe that these events are the same erratic ‘outbursting’ features that were identified by Honeycutt & Kafka (2004). We do not however, believe that these are true outbursts primarily because of the preceding drop in brightness and secondarily it would be unusual for a dwarf nova outburst of any sort to originate in the high state. LN UMa is static in colour throughout observations (see Fig. 2) with no significant change in colour index observed [mean $(g - r) = 0.02$].

LN UMa was observed in six *TESS* sectors with 120-s cadence contemporaneous with the ZTF observations. In sectors 14 and 47, we see a ~ 3 d increase in brightness; which in the sector 47 event is preceded by a decrease in brightness. The event in sector 14 has mostly symmetric temporal profile with an approximately equal rate of change of brightness in both the rise and the fall phases. The sector 47 event, in contrast, shows a rapid rise phase followed by a slower decline and appears similar to an SU UMa-type super outburst in profile. We show both events in Fig. 4.

In addition to this, each sector observed showed a periodic brightness variation. Period searching each of the sectors revealed a period, which varied by sector, of between 3 and 6 d as shown in Fig. 5. In many sectors this variation contributes the most power (or a close second) to the periodogram, more than the orbital period. In the sectors which we show in Fig. 4 this variation can be clearly seen.

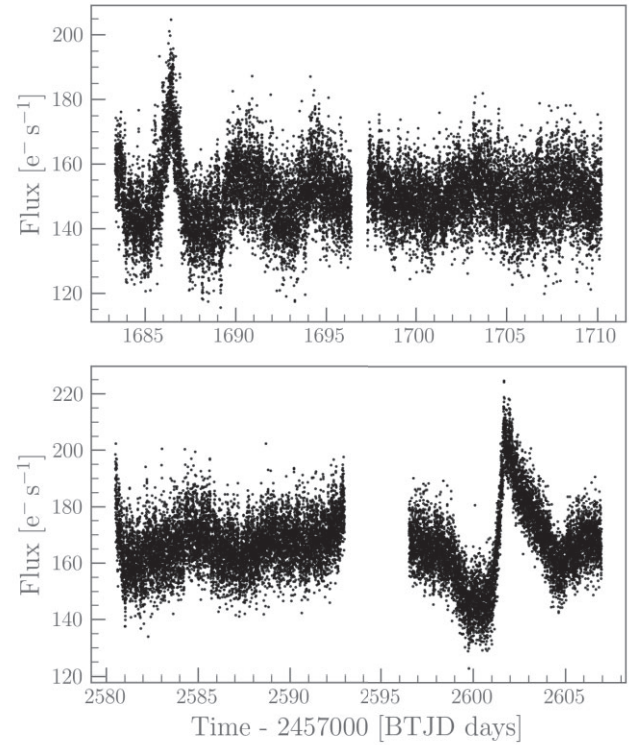


Figure 4. Extract of the *TESS* light curve showing, upper: the sector 14 event and, lower: the sector 47 events in LN UMa.

2.2.5 V794 Aql

High state observations of V794 Aql by ZTF reveal a substantial variation of up to ± 1 mag centred upon mag ~ 15 , previously highlighted by Honeycutt et al. (2014). This variation appears in both of the observed bands. Period searching on this high state variation revealed signal between 17 and 19 d. These are however, unlikely to be similar to the other period features we present in this work (Section 3.2). We consider that this feature is likely associated with

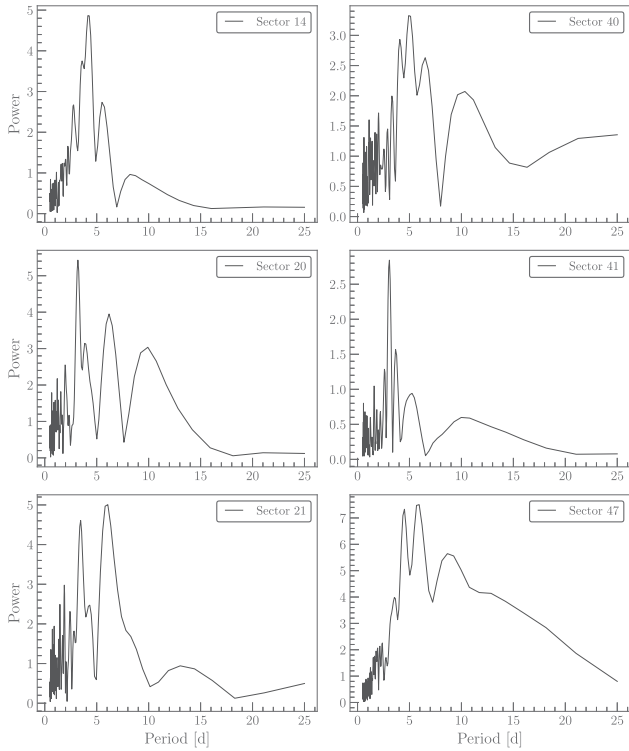


Figure 5. The Lomb–Scargle periodograms of each of the TESS sectors of LN Uma observations showing a variable period between 3 and 6 d.

the accretion disc due to its absence from observations of the low state. Indeed (Honeycutt et al. 2014) identified these features as ‘small outbursts’ which they saw to reoccur on a period of ~ 15 – 50 d, which is entirely consistent with the data we present here. A consequence of this interpretation is that we are required to reassess the value attributed to the high state brightness, setting it equal to the quiescent brightness between these features (mag ~ 16 – 17), which in turn affects any amplitude calculated (which is reflected in Table 1).

We also see two transitions into and out of relatively short lived low states, with both at minimum brightness for ~ 30 d. It is not clear if the system truly completes the transition out of the first low state, however, as though the transitions peak close to the mean high state brightness the large brightness variation does not resume. As such it is possible that V794 Aql does reach high state again only to near immediately begin another transition to a low state but alternatively it is also possible that this an abortive transition out of the low state which fails to reach the high state. The measured transition speeds are consistent with those seen in other systems lying approximately in the middle of the distribution of e -folding values which we measure. After the low state events the previously seen high state behaviour reasserts itself, however the extent of the depth of the variation increases by mag ~ 1 before gradually narrowing back to its initial behaviour. Similar to the behaviour which we report in BZ Cam, though to a greater extent, V749 Aql becomes redder at lower brightness.

2.2.6 BZ Cam

There appears to be a low state early on in the ZTF observations which unfortunately falls during a visibility gap in observations; the early

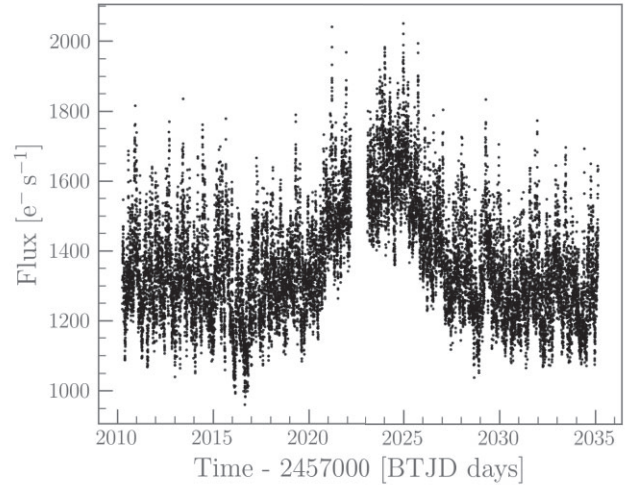


Figure 6. Extract of the TESS light curve showing the sector 26 event BZ Cam.

time data are insufficient for us to ascribe it as either part of the high state or early transition. However, observations after the visibility gap indicates the end of a transition from a low state. Other studies have identified low states occurring rarely where BZ Cam drops to a relatively shallow brightness of $V = 14.3$ mag (Garnavich & Szkody 1988; Greiner et al. 2001), which the ZTF observations are entirely consistent with. The transition we observe is by far the slowest we measure; this in part is due to the lack of data covering the entire transition although it is likely that its apparent slowness is a feature that a more complete data set would confirm. The colour distribution in BZ Cam has a relatively narrow spread, however with a clear trend to become redder at lower brightness.

The TESS observations of BZ Cam cover the high state, the majority of which show steady state behaviour. In sector 26, however, we see a ~ 80 per cent increase in brightness in an event lasting approximately 10 d, shown in Fig. 6. The event, which takes on symmetric profile, is not preceded by a dip in brightness (c.f. Section 2.2.4). Unfortunately it falls in a ZTF visibility gap so we have no complimentary data with which to compare this event, but we believe that this is perhaps a short lived increase in mass transfer rate.

2.2.7 ES Dra

ES Dra is seen in the first ~ 400 d of ZTF data at a high state of mag ~ 15 consistent with previous high state observations (Ringwald & Velasco 2012) who identified the system as a Z Cam type. Despite this, Kato (2022) identified the system as both a Z Cam and VY Scl possessing low states and transitions in which no outbursts occur. Following the initial high state we see a transition to a depth of mag ~ 17 , which is the known brightness of the low state in this system (Kato 2022). Following this singular transition, the ZTF data coverage decreases dramatically making it difficult to describe the behaviour of light curve with degree of certainty. In order to overcome this challenge, we supplemented the ZTF data with data from ATLAS (Asteroid Terrestrial-impact Last Alert System; Tonry et al. 2018). These additional data confirm the transition to a low state which is followed by a near immediate transition out of the low state, with the entire event being complete within ~ 35 d. For the transition which we were able to measure, the data quality was not sufficient to yield a usable measurement, is at the fast end of the distribution of transitions

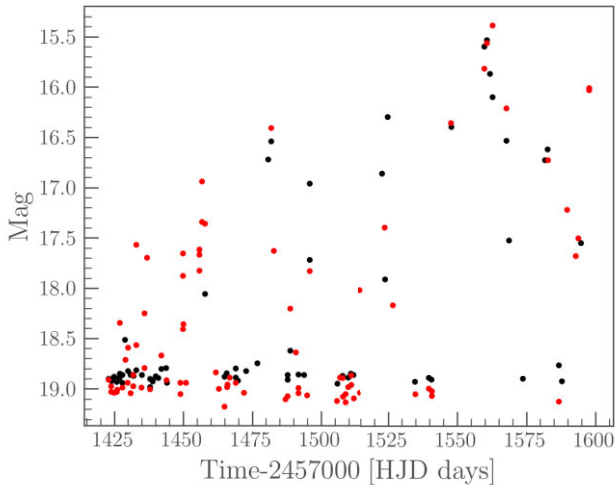


Figure 7. Extract of the ZTF *g* and *r* band, shown in black and red, respectively, of KR Aur showing the successive ‘outburst’ events approaching the event of the low state.

measured. This may be associated with the relatively shallow low state similar to the transitions in V794 Aql. Following this, and similar to the findings presented by both Ringwald & Velasco and Kato, there appears to be evidence of a dwarf nova outbursts (c.f fig. 4 Ringwald & Velasco 2012; see Fig. 1 at $T \approx 1600$, 1975) consistent with Z Cam outbursting behaviour. Like some other systems which we have discussed in this work there appears to be a preference towards reddening in the low state.

The *TESS* data for ES Dra, which are taken during the high state do not yield particularly insight to the behaviour of ES Dra, as it is spatially close to a bright solar-type variable star. As a result, much of the *TESS* data are contaminated by the flux contribution of this nearby star.

2.2.8 KR Aur

Observations of KR Aur from ZTF include two low states (mag ~ 19); the first starting before the commencement of the observations lasts for at least 500 d, while the second lasts ~ 200 d and is caught almost in its entirety. Subsequent to each low state we also observe a high state (mag ~ 14), the first lasting ~ 100 d and the second lasting at least 400 d extending past the end of observations. The transitions between the states show speeds typical for the those presented in this work, falling in the middle of the distribution; there is however a marked difference between the transition into the low state which is much faster than those where it is returning to the high state.

Approaching the end of each of the low states we observe a number of ‘outbursts’, an example of which we show in Fig. 7, the amplitude of each being greater than that which preceded it. The initial ‘outbursts’ have an amplitude of ~ 1 mag with the final ones, immediately before the onset of transition, having an amplitude of ~ 4.5 mag coming close to high state brightness. Although the sampling of the data makes it difficult to ascribe an exact duration to these events they appear to increase from ~ 10 to ~ 30 d as the brightness increases. Due to the seasonal gap in data, we are unable to confirm if these events continue up until the transition out of the first low state seen, though they are seen immediately before the transition out of the second low state. Unlike the events seen in LN UMa (Section 2.2.4) these events are associated with a change in

the colour index. The colour index increases dramatically during the ‘outbursts’ with the brighter events attracting a greater colour index, e.g. they appear to be substantially more red than stable time observations, which leaves these events at odds with typical DN outbursts and the predictions of the DIM (Hameury et al. 2020).

2.2.9 V504 Cen

The 20 s *TESS* photometry of V504 Cen reveals, as shown in Fig. 8, in addition to the orbital period, a peak in the power spectrum at four times the orbital period. This is consistent with the findings of Bruch (2022) who considered 120 s *TESS* photometry of V504 Cen. That work however was unable to attribute any physical meaning to this long period, discounting the possibility of negative superhumps due to the significant deviation from the orbital period of the system. We agree with the assessment of Bruch that this period is far too long relative to the orbital period to be a superhump, however, the exact physical origin, of this period is not at all obvious, though the absence of lower harmonics of the orbital period would appear to eliminate that as the source of this feature. We suspect, if physical, that it may be associated with some form of disc accretion. Using the relation developed by Armstrong et al. (2013, equation 1), which relates such a superorbital period to a negative superhump period, does not direct us to even a marginal peak in the power spectra indicating that indeed no superhump is present in this system.

2.2.10 MP Gem

Recently identified as a VY Scl-type system by Kato (2021), using the same ZTF data we present here, prior to this its classification was unknown. The ZTF data show a single deep low state through the middle of 2018; the first observed since 1944 (Hoffmeister 1963). The ZTF observations commence with the transition into the low state well advanced, additionally, a visibility gap arises during the low state which makes it difficult to determine the exact duration of the state and impossible to determine its true depth. We were able to mitigate this issue by supplementing the ZTF data with data from AAVSO.⁶ This helps us to constrain the duration of the low state to ~ 300 d. Due to the visibility gap it is difficult to interpret the colour data with respect to the low state; only two data points are present from the low state which makes conclusions impossible to draw and leaves open the possibility that one, or both, are outliers and as such further observation of any future low state would be needed to confirm the colour behaviour.

3 OVERVIEW OF PHOTOMETRIC FEATURES

From our study, we have identified three features that appear in VY Scl systems: low states and their associated transitions, enhanced mass transfer events, and (quasi) periodic variations. We now address these in turn.

3.1 States and transitions

Transitions into low states are the defining feature of VY Scl binaries – they are not, however, all made equal. From the initial sample of 23 systems which we considered (see Table A1), we identified only 7 which featured low state behaviour in the coverage provided by *TESS* and/or ZTF. In addition, we also see substantial differences

⁶The American Association of Variable Star Observers: aavso.org.

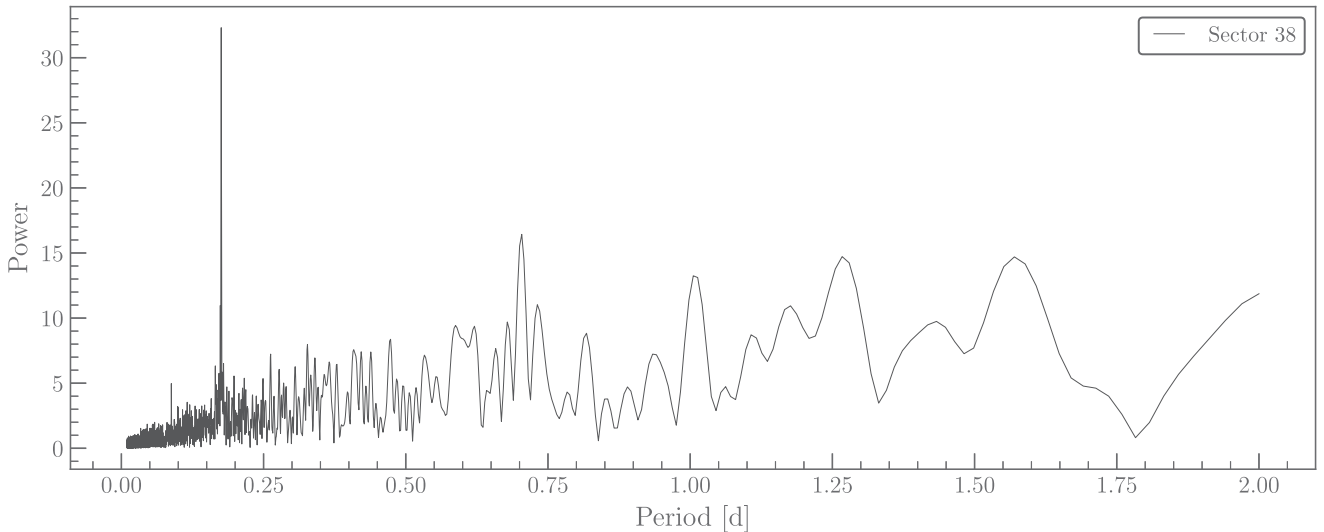


Figure 8. The Lomb–Scargle periodogram of the *TESS* observations of V504 Cen showing mostly strongly the orbital period followed by the signal at 4 times longer than the orbital period.

in how this behaviour relates to the recurrence time and duration which vary substantially. Fig. 2 shows the distributions of colours and brightness states in the ZTF systems. Restricting ourselves to just the brightness states initially, we see for example that both KR Aur and RX J2338+431 have a similar sampling and show at least one low state; however, they have strikingly different brightness distributions. KR Aur has a roughly bimodal distribution spending approximately equal amounts (~ 35 per cent per Table 1) of time in both states, with the remaining time spent at intermediate brightnesses corresponding to transitions or ‘outbursts’. RX J2338+431 in contrast strongly favours high state brightness with only a very small number of days at low state or transitions.

This pattern of variability in low state behaviour highlighted here is repeated across the sample of VY Scl systems which we present in this work, and is immediately apparent visually from Fig. 1 and is quantitatively supported by Table 1 where we see a spread in the fraction spent in the observed high state values and depth of the low states. It is, however, unclear what its physical origin of this variation is, with no apparent correlation to orbital period (which is often correlated to a variety of system parameters in CVs).

In Table 2, we show the e -folding time for each of the transitions which we have observed. This shows that the transition speeds generally fall within a broad range, 16.7–33.5 d, with a few outside this range. The distribution of the speed of transition appears to have no association with the measured orbital period of the system; there is a weak correlation between the depth of the transition and its speed with deeper transitions being slower in general – although this discounts BZ Cam which has a very slow but apparently shallow transition. This could be understood in the context of deeper transitions arising in systems where the disc is a larger contributor to the overall brightness and therefore physically larger. In this circumstance a physically larger disc would likely shrink or dissipate more slowly than a smaller disc. We also see that the fastest transitions occur in those systems which almost immediately transition out of their low state instead of remaining in a sustained low state, this suggests that some ‘inertia’ exists in the mechanism which suppresses mass accretion – the longer it is in place the more established it becomes.

Within individual systems the speed of transitions are more consistent; however, we observe that there is an appreciable difference

between the speeds into low state and out of low state transitions. Continuing in the spirit of these systems behaving differently to each other, we see that two of the systems show faster transition into the low state, whereas three systems are faster when leaving the low state. There is no relationship between such systems and the orbital period of the system, similarly the amplitude of the transitions appears to show no correlation with these behaviours. As there appears to be no theoretical predictions surrounding the speed of the transitions it is difficult to ascertain if there is a genuine physical process at work due to the relatively small numbers considered in this work. Despite this, given that we observe in those systems which have more than a single pair of transitions a consistency in behaviour, suggesting it is probable that this is not an artefact of a selection bias but a real feature.

Turning to the variation in the colour of the systems between high and low states, we see that once again there is no one single behaviour observed in these systems, with differences between both high and low states seen across multiple systems. We see in at least three systems a preferential reddening at lower brightness, whilst the remaining appear to show no difference in colour between the different states. In addition to this, we see that for *all* systems during their respective high states that there is a positive correlation between brightness and blueness; this is entirely inline with expectation as within a high state brightness variations associated with small changes in the mass transfer rate would be expected and slight increases would increase both the brightness and the temperature of the system, hence the observed blueness relation.

3.2 Periodic behaviours

Three of the systems which we have discussed appear to show periodic variations in their light curve which are identified by the high-time resolution made available to us by *TESS*. A number of periodic behaviours have been identified previously in CVs in addition to the orbital and spin periods (Table 1) of the systems. These include positive and negative superhumps, superorbital periods, and the associated beats and harmonics that arise from the interaction of these periods. Superhumps have frequencies within a few per cent of the orbital period: physically negative superhumps are associated with a warped accretion disc which has a retrograde precession in the

inertial frame (Thomas & Wood 2015), whilst positive superhumps are associated with a resonant tidal stress in the accretion disc induced by the secondary star driving a ‘flexing’ disc oscillation in the orbital plane and a positive precession in the inertial frame (Whitehurst & King 1991; Wood, Montgomery & Simpson 2000). The periods of precession (retrograde and/or prograde) are called superorbital periods, and can make an additional contribution to the power spectrum of a given system over and above what might be expected from the interaction of the superhump and orbital period (Armstrong et al. 2013).

The *TESS* light curve of LN UMa varies on a substantially longer time-scale than any of the other systems that we have presented, with a frequency well below 1 d^{-1} which varies depending on the sector considered; giving periods between 3 and 6 d. Placing this even further at odds with the other systems this very low frequency variation is often the dominant frequency in the light curve such that it can be easily picked out by eye in the light curve (see Figs 4 and 5). If this is a superorbital period associated with the disc precession then it indicates both a very slow precession which makes a substantial contribution to the flux of the system.

4 DISCUSSION

4.1 Light curve morphology dichotomy

The high mass transfer rate during their high state and the lack of outbursts in the low state are common properties of all VY Scl systems (Warner 2003). We argue that these common features indicate the presence, or absence, of certain mechanisms intrinsic to these CVs. However, there are also observational features found in some but not all VY Scl systems. For instance, from the visual inspection of the light curves shown in Fig. 1, we may broadly divide them into two sub-groups based upon their brightness variations⁷: (i) systems with a relatively weak brightness fluctuations in their light curves in high states (Group A systems), and (ii) systems with substantial flickering in the light curves in high states (Group B systems). With this in mind, we now attempt to construct a framework, in terms of mass transfer, accretion in interacting binaries and the feedback reaction to mass transfer processes and the orbital dynamics, to account for the phenomena associated with the high–low states observed in the VY Scl binaries in a holistic matters.

The most noticeable feature of the Group A systems is that there is a brightness ceiling during the high states. Moreover, the low states are episodic, where the brightness either drops dramatically from the ceiling brightness, e.g. in RX J2338+431 and ES Dra, or the source becoming substantially dimmer for a reasonable long duration, e.g. in MV Lyr, KR Aur, and MP Gem. The light curves of the Group B systems are complex and structured and appear not to have a brightness ceiling during the high state. They, however, exhibit flare-like fluctuations in the high state, e.g. in LN UMa. Although the entry and the exit of the low states in some systems, e.g. V794 Aql, can be identified, the brightness variations during the state transitions in the other systems are not easily characterised.

⁷We define this by setting DM as the difference between the magnitudes of the low and the high state and dm as the variation of the magnitude of the source during their high state. For MV Lyr, $DM = 5$ and $dm < 1$; and for V794 Aql $DM = 4$ and $dm = 2$. Thus, $dm/DM < 0.2$ for MV Lyr and $dm/DM 0.5$. Therefore, MV Lyr has relatively weak fluctuations in the high state and V794 Aql has substantial fluctuations in the high state

4.2 Scenarios on high–low states and state transitions

The high and low states in CVs are often attributed to the high and low rates of mass transfer from the mass donating star to the WD. This association may be appropriate for magnetic CVs, such as Polars and Intermediate Polars (Duffy et al. 2022; Mason et al. 2024), but problematic when the binary has a fully developed accretion disc.

In CVs, the secular mass transfer rate averaged over episodes of high and low states, are determined by the efficiency of angular momentum loss (see e.g. Verbunt & Zwaan 1981). The high-mass transfer rates in VY Scl binaries, relative to other CVs with similar orbital parameters, therefore requires additional mechanisms that increase the loss or transfer of angular momentum from the orbit to the component stars.

Observations have shown that VY Scl binaries are more often in the high state than in the low state. Moreover, their high brightness in the high states cannot be merely due to stability in the accretion disc, implying that the mass transfer also occurs at a very high rate in the VY Scl binaries (see Zemko et al. 2014). The two pieces of observational evidence must be accounted for when building a model to explain secular behaviour of VY Scl binaries.

While the high state of VY Scl binaries are often attributed with the accretion-disc instabilities (see e.g. Mineshige 1993, for a review of disc instability), the state transitions are triggered by the change in the mass outflow from the companion star (see King & Cannizzo 1998). Changes in the mass transfer in CVs can be caused by activity intrinsic to the companion star, such as stellar magnetism, or certain external processes, such as certain interactions between the companion star and the WD. The companion star in CVs are low-mass stars which can show evidence of strong magnetospheric activity (see Berdyugina 2005). The migration of multiple magnetic star-spots or a giant star-spot into the region near the L1 point will alter the outflow of material from the donor secondary star (Livio & Pringle 1994) which is filling its critical Roche surface. The magnetic fields carried by the star-spot(s) into the L1 region, depending on the orientation, can create a barrier blocking the flow of material through the L1 point into the WD’s Roche lobe. Mass transfer resumes when the star-spot(s) migrate out the L1 region. This process is magnetohydrodynamical (MHD), not directly associated with the evolutionary state companion star (which is of the longer Kelvin–Helmholtz time-scale), the orbital dynamics of the binary, or the physical condition of the accreting WD.

Despite being appealing, the star-spot scenario does not explain the prolonged low state as observed in some systems, e.g. KR Aur. Inspection of the light curves of the Group A systems (see Section 4.1) also reveals that their brightness does not show large-amplitude brightness flickering, when they enter the low state. Plasma and MHD processes generally exhibit instabilities, which can trigger flaring and eruptive behaviour, which would be seen as flickering. Therefore, the mass transfer in these VY Scl binaries is either absent or relatively steady during the low state. This also hints at the presence of some secular processes, at least partially responsible for, driving the Group A systems into the low state, and these driving processes are relatively steady, evolving over time-scales significantly longer than the duration of the high–low state and their transitions. Migrations of magnetic star-spots of the companion star are on relatively short time-scales and therefore are unlikely to drive the Group A systems from a high state or confine them in a prolonged low state.

As opposed to the star-spot scenario, the high state is now not necessarily the default state, and the low state is not simply a temporary disruption of the mass transfer. This puts the high and low states in a similar footing in the modelling, where the average

mass transfer is driven by the secular orbital evolution, with magnetic braking and/or gravitational radiation as the angular momentum loss mechanisms (see e.g. Verbunt & Zwaan 1981). It should be noted however, the understanding of the drivers of secular orbital evolution are not completely understood as there is strong irradiation of the M star which could give rise to non-linear feedback (see Wu et al. 1995)

4.3 A more holistic consideration

Leach et al. (1999) and Hameury & Lasota (2002) present explanations as to the absence of disc instability in VY Scl systems, but are markedly different, relying on entirely different physics to arrive at their conclusions – Leach et al. (1999) uses disc irradiation whereas Hameury & Lasota (2002) relies upon weak WD magnetism eliminating the accretion disc.

Due to the weakness of the proposed magnetic fields required by Hameury & Lasota’s model and the data that we have considered in this work, we cannot address this theory directly; had we had *TESS* data of low states it may have been possible to confirm the presence of a disc by identifying periodic features originating from a disc. Despite this it remains part of our consideration throughout this work. We can however address the disc irradiation model with the present data.

The disc irradiation model states that during the low state the WD is sufficiently hot to irradiate the inner accretion disc such that it can have a temperature which would ordinarily be associated with the stable high state. As the system is substantially fainter in this configuration, we would anticipate that the relative contribution of the irradiated disc to the total brightness would increase. Under this scenario, the irradiated disc, having remained hot, should produce a greater blue excess than would be expected for a system in a low state, which may manifest as simply not seeing an increase in red excess. Consequently, we believe that those VY Scl stars which do not become redder during their low state are showing evidence of an irradiated inner disc.

As noted previously the colour behaviour during low states is not a universal behaviour, with many of the systems becoming redder during the low state. Continuing with the hypothesis that colour evolution can be used as a tracer of an irradiated disc, this would imply that these systems lack such a disc, and as noted by Hameury & Lasota (2005) some cases exist (including MV Lyr) where the weak magnetic field model successfully holds at the expense of the disc irradiation model. Without being able to probe the weak magnetic field model with the data presented here we cannot comment directly on its validity, however comparing our data with that discussed in Hameury & Lasota (2005) we see no grounds for disagreement. With this in mind we believe that *both* models are valid and apply to systems according to the colour behaviour which they exhibit. We further believe that this is the case because it seems unlikely that all of the WDs across the VY Scl binary population are magnetic, first because we (and others) have seen evidence for ‘outburst’ like behaviour most plausibly originating in a disc and secondly because WD population studies seeking magnetism below the threshold required for magnetic disc disruption have identified a substantial fraction of the population are not magnetic (Bagnulo & Landstreet 2021).

The other challenge of the behaviour in VY Scl binaries is understanding why during the transitions we do not observe outbursts, as these generally take longer than the viscous time. Whilst the magnetic model is capable of eliminating the disc for a sufficient duration to explain the absence of outbursts, the disc irradiation model has more difficulty. As the disc grows with increasing mass transfer rate during

the transition it becomes increasingly difficult for irradiation to keep the disc hot enough to prevent instability developing (the reverse of this issue applies during transitions into low states). If we consider the transitions of those systems which we believe to be disc irradiation systems with those likely governed by magnetism we see that there is no discernible relationship between the colour behaviour and the speed, τ , or the duration of the transitions. With that being the case we do find that the shortest mean duration for transitions is in those systems which are preferentially red in the low state however, this does not extend to all such systems. Consequently, we do not believe that this can offer any explanation as to the transition behaviour which we observe.

As we have already highlighted, there is a wide range of transition speeds and low state durations present in the VY Scl binaries we have considered here. We see in those systems with the shortest low states, e.g. RX J2338+432 and ES Dra, that these systems have the fastest transitions which we measured. Similarly, we see in those systems with much longer low states, e.g. MV Lyr and MP Gem; that these systems generally have far slower transitions. Although there are some exceptions to this, for example KR Aur where other factors may be involved (see Section 4.4), there does appear to be a correlation between the speed of transition, which may be connected to the aforementioned weak correlation between transition speed and state depth as longer low states tend to be deeper. This indicates that there exists a difference in the mechanism of the transitions in shorter shallower low states from those longer deeper low states.

4.4 Enhanced mass transfer

Although the absence of outbursts is a defining feature of VY Scl binaries we present evidence of ‘outbursts’ or enhanced mass transfer events. This would not be the first time such events have been seen in VY Scl binaries with previous observations of magnetically gated outbursts (Scaringi et al. 2017) and ‘stunted outbursts’ (Honeycutt & Kafka 2004). The events which we observe, however, are diverse in nature and with the exception of V794 Aql, do not appear to have been previously identified and seem to be different from those which been remarked upon before.

Like the stunted outbursts seen in V794 Aql, the events which we see in LN UMa, have a quasi-periodic nature, with a similar duration and recurrence time, which indicates that it is appropriate to identify them as ‘stunted outbursts’. The LN UMa events however have some key differences, first they are not ubiquitous to the high state; indicating that the instability which causes them is not permanent. Furthermore, unlike V794 Aql the events in LN UMa are not symmetric and always commence with a fall in brightness before entering a rise phase. This indicates that mass transfer is (partially) disrupted for a short time before increasing above the normal high state rate. This suggests that when mass transfer is disrupted the mass that ordinarily flows during this time builds up at some boundary before being released resulting in an enhanced rate and consequently brightness. It is likely that the physical origin of these events are linked through mass transfer instability, with LN UMa having an additional contribution from the magnetic field causing the mass to be held at some boundary (c.f. magnetic gating; D’Angelo & Spruit 2010, 2012).

The events we present in KR Aur are particularly interesting, with parameters which appear to be directly tied to the imminence of a transition to the high state. These ‘outbursts’ get progressively greater in amplitude (1.5–4.7 mag) and redder (0.15–0.70) in colour as the system nears transition. This implies that physically these events involve material that is locally cooler than the rest of system. If, as

we suggest in Section 4.2, KR Aur is a system that has a disc, it is possible that these events indicate an increase in the mass transfer rate from the L1 region which results in only part of the accretion disc being inflated in size and brightness before fading again as material dissipates returning to the quiescent brightness. As the mass transfer rate continues to increase so does the scale of the events until the mass transfer rate is sufficient to trigger an all disc effect – transition back to the high state. Physically, this may be an extreme case of the flaring observed in the low state of the group A systems (see Section 4.5), which induces some feedback mechanism to inflate the buffer annulus.

The final remarkable event which we have observed is the relatively long outburst observed in BZ Cam. Lasting ~ 10 d and with a relatively small increase in flux this is indicative of a stunted outburst. With the *TESS* coverage that is available we would ordinarily expect to identify more than one such event, however without consecutive sectors of observation and allowing for a low recurrence time there are many plausible recurrence time-scales where we would miss subsequent events. That explanation is not satisfactory to explain the apparent absence in ZTF data. It is possible that these events are hidden in the stochastic variation of the high state light curve (which is at the upper range of ZTF's capability), although the flux increase seen in the *TESS* data indicates that this may be unlikely. Revisiting the light curve, there are occasions (e.g. HJD ≈ 2458500 and HJD ≈ 2459150) where the brightness exceeds the local neighbouring values – it is possible that these are further events that we simply cannot resolve. Unfortunately, these events occur during gaps in the *TESS* coverage; however, if we assume that these are similar events then combined with the resolved event we see a recurrence time-scale of $\gtrsim 100$ d. Subsequent AAVSO data would appear to support this, with at least two similar events present (e.g. JD ≈ 2459000 and JD ≈ 2459630). This most likely cannot be definitively addressed without more long term observations which are suited to detecting such brightness changes in relatively bright sources.

4.5 A phenomenological model for the brightness variations and brightness ceiling in the high state

The apparent ceiling of the brightness of the Group A system implies their maximum brightness is determined by a set of variables that are relatively stable and do not vary over short time-scales. One possibility is the formation of an optically thick annulus boundary layer with a small width attaching to the WD. The outer boundary of the opaque boundary layer contacts a buffer annulus, which acts as a mass reservoir and regulates the inflow of the material into the inner opaque boundary layer. The maximum brightness is therefore determined by the temperature and the size of ‘photosphere’ corresponding to this boundary layer, which are determined by the mass and radius of the accreting WD. The high state therefore corresponds to the situation where the buffer annulus is filled and the low state corresponds to the situation where the buffer annulus is empty. Moreover, the radiative force must play an important role, and the flows there are thermally stable (absence of cooling induced instability), weakly magnetic (avoiding eruptive magnetic reconnection), and non-convective (allowing laminar circular flow).

In this scenario flaring can occur during low states, where the buffer is almost empty and the optically thick annulus boundary layer cannot be formed. The magnetic activity and hydrodynamic instability in the resident flow can trigger flares. In a certain way, the structure of the disc is analogous to a solar-like star but in 2D, where an radiative inner region is bounded by a convective outer region.

The Group B systems are those where the optically thick radiative dominate annulus boundary layer cannot form. A possibility is that the WDs in the Group B systems have a strong magnetic field, which have non-uniform strengths and orientation distributions over the WD surface. The magnetic field causes instability, disrupts the flow, and the optically thick annulus boundary layer; hence the buffer annulus outside it cannot be developed. The high–low states of the Group B systems are triggered by the variations in the secular mass transfer, and the flaring simply reflects the instability in the flow triggered by the magnetic field in the accretion disc which also interacts with the magnetic field of the WD. This scenario can also easily accommodate the observations that some VY Scl binaries show behaviour similar to that of supersoft source (see Greiner et al. 2010) and that a strong wind can be launched from the disc of VY Scl binaries (Inight et al. 2022).

The remaining questions are now how to maintain the high state of VY Scl in Group A and how to model the respective accretion discs in the Group A and Group B systems. One scenario to explain systems which can sustain high-mass transfer rate (during the high states) above the average mass transfer rate set by orbital evolution due to angular momentum loss is irradiative heating of the mass donor star (see e.g. Wu et al. 1995). This is easier to achieve in the Group A systems as their high states tend to have a stable ceiling luminosity from the radiative dominate flow near the WD. The answer to the latter question is less trivial. It will require a more sophisticated accretion disc model that can take care of the complex interaction between magnetic field interaction within the accretion disc and between the WD and the accretion disc together with relevant radiative hydrodynamics processes self-consistently.

4.6 Remarks on the periodic behaviours

We see three different manifestations of notable periodic behaviour in the systems we have considered in this work; a 1.1 d period in TT Ari, a $\sim 4P_{\text{orb}}$ period in V504 Cen, and a ~ 3 –6 d period in LN UMa. The variety of features observed indicates a diversity in the physical properties of the systems. Whilst the period in TT Ari can be explained reasonably simply (see Section 3.2) such that may be seen in any CV with an accretion disc, the others are more puzzling. As stated previously the periodic signal in V504 Cen cannot be either a superhump nor a superorbital period; however it is clearly real as it exists in two separate data products. As we have previously suggested, it may be some resonant accretion feature where the mass transfer rate varies on the time-scale of the observed variation. A concerted observational effort will be required to establish the exact origin of this feature is and would benefit from study from a longer term view point in addition to that provided by *TESS*.

Finally, we turn to LN UMa, which shows a very prominent low frequency oscillation that appears to change over relatively short time frames – although it is possible that we are detecting a harmonic or overtone of a single frequency. Nevertheless, without needing to ascribe an exact value to this period, we can say that this period almost certainly is real, but of unclear physical origin. If LN UMa is a system with high inclination,⁸ it is possible that the inclination is generating some projection effect that affects the fraction of the accretion spot that can be seen, however we would expect that this would occur on a period that could be related reasonably easily to

⁸No value for the inclination of LN UMa is available, however as a member of the SW Sex sub-class it is reasonable to assume that this is the case (Gänsicke 2005).

the orbital period. In order to fully understand this feature further, study will be necessary including an effort to determine if the period is fixed or not, and if not what the rate of period change \dot{P} is.

Unusual periods in CVs with physical origins that cannot immediately be identified is not an unheard of phenomenon. Bruch (2022) who studied the long term *TESS* light curves of 15 different CVs (including three systems we consider here) found several unusual but none the less real periodicities. For example in AC Cnc they identify a 4.6 d period which they cannot identify an origin for. In V533 Her they identify variations in the superhump periods, in this case they ascribe the variability to interactions between different periods of different amplitudes. That work concludes that systems which have unusual periodic behaviours should be subject to concerted high cadence study with complimentary follow-up observations to understand system parameters which may be useful in understanding the physical origin of these periods.

5 CONCLUSIONS

Although a relatively small sub-class of Nova-like CVs, the fact that VY Scl systems show irregular drops in brightness of over 1 mag shows they are important sources with which to understand how the mass transfer rate in accreting binaries is regulated. Similar to other Nova-like systems, VY Scl systems do not show classical outbursts, however they do show low states. Additionally the DIM predicts outbursts should be seen during the low states (if a disc is present), though the ‘outbursts’ which are present cannot be supported by the DIM. These outbursts have a range of behaviours including those of KR Aur which are repeated and become increasingly energetic throughout a low state. Further examples of stunted outbursts, such as those we present here, in VY Scl and other systems can help give further insight to their cause.

Having presented long baseline and high time resolution observations of 10 known VY Scl systems, we have reviewed the models which set-up to describe the behaviours of these systems and attempted to reconcile these with observations. We have presented a unified model to describe both the cause of the state transitions and the observed variability of VY Scl systems light curves and how this differs on a system to system basis.

The observations shown here have, at least in part, come from all-sky optical surveys. With the expansion of surveys, with some projects such as GOTO (Dyer et al. 2022; Steeghs et al. 2022) having telescopes in the Northern and Southern Hemispheres, with the capacity to cover the entire sky every few days, the opportunity exists to greatly extend our length of coverage of VY Scl systems to gain a better long term view of their accretion behaviour. In particular, it will be possible to obtain multiwavelength spectroscopy of sources which go into a new accretion state or which start a series of stunted outbursts. This will give essential information with which to improve accretion instability models to account for their behaviour.

ACKNOWLEDGEMENTS

This paper includes data collected by the *TESS* mission. Funding for the *TESS* mission is provided by the NASA Science Mission Directorate.

It also includes ZTF data obtained with the Samuel Oschin Telescope 48-inch and the 60-inch Telescope at the Palomar Observatory as part of the Zwicky Transient Facility project. ZTF is supported by the National Science Foundation under grants Nos AST-1440341 and AST-2034437 and a collaboration including current partners Caltech, IPAC, the Weizmann Institute for Science, the Oskar Klein Center

at Stockholm University, the University of Maryland, Deutsches Elektronen-Synchrotron, and Humboldt University, the TANGO Consortium of Taiwan, the University of Wisconsin at Milwaukee, Trinity College Dublin, Lawrence Livermore National Laboratories, IN2P3, University of Warwick, Ruhr University Bochum, Northwestern University and former partners the University of Washington, Los Alamos National Laboratories, and Lawrence Berkeley National Laboratories. Operations are conducted by COO, IPAC, and UW.

This work has also made use of data from the Asteroid Terrestrial-impact Last Alert System (ATLAS) project. The Asteroid Terrestrial-impact Last Alert System (ATLAS) project is primarily funded to search for near Earth asteroids through NASA grants NN12AR55G, 80NSSC18K0284, and 80NSSC18K1575; byproducts of the NEO search include images and catalogues from the survey area. This work was partially funded by Kepler/K2 grant J1944/80NSSC19K0112 and HST GO-15889, and STFC grants ST/T000198/1 and ST/S006109/1. The ATLAS science products have been made possible through the contributions of the University of Hawaii Institute for Astronomy, the Queen’s University Belfast, the Space Telescope Science Institute, the South African Astronomical Observatory, and The Millennium Institute of Astrophysics (MAS), Chile.

This work was funded by UKRI grant (ST/T505936/1). For the purpose of open access, the authors have applied a creative commons attribution (CC BY) licence to any author accepted manuscript version arising. CD acknowledges STFC for the receipt of a postgraduate studentship.

Armagh Observatory & Planetarium is core funded by the Northern Ireland Executive through the Department for Communities.

This work made use of ASTROPY:⁹ a community-developed core PYTHON package and an ecosystem of tools and resources for astronomy (Astropy Collaboration 2013, 2018, 2022).

This research made use of LIGHTKURVE, a PYTHON package for Kepler and *TESS* data analysis.

We acknowledge with thanks the variable star observations from the AAVSO International Database contributed by observers worldwide and used in this research. This work has made use of the NASA ADS.

DATA AVAILABILITY

TESS data are available from the Mikulski Archive for Space Telescopes (MAST), which can be accessed at <https://mast.stsci.edu/portal/Mashup/Clients/Mast/Portal.html>

ZTF data are available via the NASA/IPAC Infrared Science Archive <https://irsa.ipac.caltech.edu/Missions/ztf.html>

ATLAS forced photometry data are available from the collaboration website <https://fallingstar-data.com/forcedphot/>

REFERENCES

- Armstrong E. et al., 2013, *MNRAS*, 435, 707
- Astropy Collaboration, 2013, *A&A*, 558, A33
- Astropy Collaboration, 2018, *AJ*, 156, 123
- Astropy Collaboration, 2022, *ApJ*, 935, 167
- Bagnulo S., Landstreet J. D., 2021, *MNRAS*, 507, 5902
- Bellm E. C. et al., 2019, *PASP*, 131, 018002
- Berdyugina S. V., 2005, *Living Rev. Sol. Phys.*, 2, 8
- Bruch A., 2019, *MNRAS*, 489, 2961
- Bruch A., 2022, *MNRAS*, 514, 4718

⁹<http://www.astropy.org>

Cannizzo J. K., 1993, in Craig W. J., ed, *Accretion Disks in Compact Stellar Systems*. World Scientific Publishing Co., Singapore, p. 6

D’Angelo C. R., Spruit H. C., 2010, *MNRAS*, 406, 1208

D’Angelo C. R., Spruit H. C., 2012, *MNRAS*, 420, 416

Duffy C., Ramsay G., Wu K., Mason P. A., Hakala P., Steeghs D., Wood M. A., 2022, *MNRAS*, 516, 3144

Dyer M. J. et al., 2022, in Marshall H. K., Spyromilio J., Usuda T., eds, *Proc. SPIE Conf. Ser. Vol. 12182, Ground-based and Airborne Telescopes IX*. SPIE, Bellingham, p.121821Y

Gänsicke B. T., 2005, in Hameury J. M., Lasota J. P., eds, *ASP Conf. Ser. Vol. 330, The Astrophysics of Cataclysmic Variables and Related Objects*. Astron. Soc. Pac., San Francisco, p. 3

Gänsicke B. T., Sion E. M., Beuermann K., Fabian D., Cheng F. H., Krautter J., 1999, *A&A*, 347, 178

Garnavich P., Szkody P., 1988, *PASP*, 100, 1522

Greiner J. et al., 2001, *A&A*, 376, 1031

Greiner J., Schwarz R., Tappert C., Mennickent R. E., Reinsch K., Sala G., 2010, *Astron. Nachr.*, 331, 227

Hameury J. M., 2020, *Adv. Space Res.*, 66, 1004

Hameury J. M., Lasota J. P., 2002, *A&A*, 394, 231

Hameury J.-M., Lasota J.-P., 2005, preprint (astro-ph/0506382)

Hameury J. M., Knigge C., Lasota J. P., Hamsch F. J., James R., 2020, *A&A*, 636, A1

Hillwig T. C., Robertson J. W., Honeycutt R. K., 1998, *AJ*, 115, 2044

Hoffmeister C., 1963, *Astron. Nachr.*, 287, 169

Honeycutt R. K., 2001, *PASP*, 113, 473

Honeycutt R. K., Kafka S., 2004, *AJ*, 128, 1279

Honeycutt R. K., Robertson J. W., Turner G. W., 1998, *AJ*, 115, 2527

Honeycutt R. K., Kafka S., Robertson J. W., 2014, *AJ*, 147, 10

Inight K. et al., 2022, *MNRAS*, 510, 3605

Kato T., 2021, preprint (arXiv:2111.07241)

Kato T., 2022, preprint (arXiv:2205.00632)

King A. R., Cannizzo J. K., 1998, *ApJ*, 499, 348

Leach R., Hessman F. V., King A. R., Stehle R., Mattei J., 1999, *MNRAS*, 305, 225

Lightcurve Collaboration, 2018, *Astrophysics Source Code Library*, record ascl:1812.013

Linnell A. P., Szkody P., Gänsicke B., Long K. S., Sion E. M., Hoard D. W., Hubeny I., 2005, *ApJ*, 624, 923

Livio M., Pringle J. E., 1994, *ApJ*, 427, 956

Lomb N. R., 1976, *Ap&SS*, 39, 447

Lubow S. H., Shu F. H., 1975, *ApJ*, 198, 383

Mason P. A. et al., 2022, *ApJ*, 938, 142

Mason P. A. et al., 2024, *ApJ*, 965, 96

Medina Rodriguez A. L., Zharikov S., Kára J., Wolf M., Agishev A., Khokhlov S., 2023, *MNRAS*, 521, 5846

Mineshige S., 1993, *Ap&SS*, 210, 83

Mizusawa T. et al., 2010, *PASP*, 122, 299

Papadaki C., Boffin H. M. J., Stanisev V., Boumis P., Akras S., Sterken C., 2009, *J. Astron. Data*, 15, 1

Patterson J., Patino R., Thorstensen J. R., Harvey D., Skillman D. R., Ringwald F. A., 1996, *AJ*, 111, 2422

Ricker G. R. et al., 2015, *J. Astron. Telesc. Instrum. Syst.*, 1, 014003

Ringwald F. A., Velasco K., 2012, *New Astron.*, 17, 108

Scargle J. D., 1982, *ApJ*, 263, 835

Scaringi S., Maccarone T. J., D’Angelo C., Knigge C., Groot P. J., 2017, *Nature*, 552, 210

Schmidtobreick L., Mason E., Howell S. B., Long K. S., Pala A. F., Points S., Walter F. M., 2018, *A&A*, 617, A16

Shafter A. W., 1983, *ApJ*, 267, 222

Skillman D. R., Patterson J., Thorstensen J. R., 1995, *PASP*, 107, 545

Steeghs D. et al., 2022, *MNRAS*, 511, 2405

Thomas D. M., Wood M. A., 2015, *ApJ*, 803, 55

Tonry J. L. et al., 2018, *PASP*, 130, 064505

Verbunt F., Zwaan C., 1981, *A&A*, 100, L7

Warner B., 2003, *Cataclysmic variable stars*. Cambridge Univ. Press, Cambridge

Weil K. E., Thorstensen J. R., Haberl F., 2018, *AJ*, 156, 231

Whitehurst R., King A., 1991, *MNRAS*, 249, 25

Wood M. A., Montgomery M. M., Simpson J. C., 2000, *ApJ*, 535, L39

Wood M. A., Thomas D. M., Simpson J. C., 2009, *MNRAS*, 398, 2110

Wu K., Kiss L. L., 2008, *A&A*, 481, 433

Wu K., Wickramasinghe D. T., Warner B., 1995, *PASA*, 12, 60

Wu X., Li Z., Ding Y., Zhang Z., Li Z., 2002, *ApJ*, 569, 418

Zemko P., Orio M., Mukai K., Shugarov S., 2014, *MNRAS*, 445, 869

APPENDIX A: COMPLETE LIST OF CONSIDERED SOURCES

Table A1. Complete list of the sources considered for inclusion in this work, showing the survey(s) in which data were available at the point of analysis. Systems were excluded from analysis where they did not show state transitions or other features of interest.

Object name	ZTF	TESS	Included for analysis
V504 Cen	×	✓	✓
VY Scl	×	×	×
VZ Scl	×	×	×
V1082 Sgr	×	×	×
V442 Oph	×	×	×
V794 Aql	✓	×	✓
LX Ser	✓	✓	×
KR Aur	✓	×	✓
RXJ2338+431	✓	✓	✓
MV Lyr	✓	✓	✓
V751 Cyg	×	×	×
BH Lyn	✓	✓	×
V425 Cas	✓	✓	×
LN UMa	✓	✓	✓
BZ Cam	✓	✓	✓
HS0506+7725	×	×	×
TT Ari	×	✓	✓
DW UMa	×	×	×
MASTER	×	×	×
OTJ190519.41+301524.4			
RX J2338+431	✓	✓	✓
MACHO 311.37557.169	×	×	×
MP Gem	✓	×	✓
ES Dra	✓	×	✓
LkHA 170	✓	✓	×

This paper has been typeset from a \LaTeX file prepared by the author.